Title	Atomistic analysis of radiative recombination rate, Stokes shift, and density of states in c-plane InGaN/GaN quantum wells
Authors	McMahon, Joshua M.;Tanner, Daniel S. P.;Kioupakis, Emmanouil;Schulz, Stefan
Publication date	2020-05-07
Original Citation	McMahon, J. M., Tanner, D. S. P., Kioupakis, E. and Schulz, S. (2020) 'Atomistic analysis of radiative recombination rate, Stokes shift, and density of states in c-plane InGaN/GaN quantum wells', Applied Physics Letters, 116(18), 181104 (5pp). doi: 10.1063/5.0006128
Type of publication	Article (peer-reviewed)
Link to publisher's version	10.1063/5.0006128
Rights	© 2020, the Authors. Published under license by AIP Publishing. This article may be downloaded for personal use only. Any other use requires prior permission of the author and AIP Publishing. This article appeared as: McMahon, J. M., Tanner, D. S. P., Kioupakis, E. and Schulz, S. (2020) 'Atomistic analysis of radiative recombination rate, Stokes shift, and density of states in c-plane InGaN/GaN quantum wells', Applied Physics Letters, 116(18), 181104 (5pp), doi: 10.1063/5.0006128, and may be found at https://doi.org/10.1063/5.0006128
Download date	2024-04-25 12:36:16
Item downloaded from	https://hdl.handle.net/10468/9946

Joshua M. McMahon (ID), Daniel S. P. Tanner, Emmanouil Kioupakis (ID), and Stefan Schulz (ID)

View Online   Export Citation   CrossMark

ARTICLES YOU MAY BE INTERESTED IN

Atomistic analysis of radiative recombination rate, Stokes shift, and density of states in *c*-plane InGaN/GaN quantum wells

View Online   Export Citation   CrossMark

Joshua M. McMahon,[1,2,a)] (iD) Daniel S. P. Tanner,[1] Emmanouil Kioupakis,[3] (iD) and Stefan Schulz[1] (iD)

AFFILIATIONS

[1]Tyndall National Institute, University College Cork, Cork T12 R5CP, Ireland
[2]Department of Physics, University College Cork, Cork T12 YN60, Ireland
[3]Materials Science and Engineering Department, University of Michigan, 2300 Hayward St., Ann Arbor, Michigan 48109, USA

[a)]Author to whom correspondence should be addressed: joshua.mcmahon@tyndall.ie

ABSTRACT

Recent experimental studies have revealed an unusual temperature dependence of the radiative recombination rate in polar InGaN/GaN quantum wells. We show, by direct atomistic evaluation of the radiative recombination rate, that the experimentally observed trend of an increasing rate with increasing temperature results from the population of energetically higher lying electron and hole states with dipole matrix elements larger than those of the band edge states relevant to low temperature studies. Given that the overall evolution of this recombination rate is tightly linked to the energetic distribution of localized states, we investigate the hole density of states and absorption spectra. Based on the calculated absorption spectra, Stokes shift energies are extracted for InGaN quantum wells with In contents ranging from 5% to 25%. Here, good agreement with experimental literature results is found. We provide also hole tail state characteristic energies as a function of the In content, a quantity that indicates the localization character of the ensemble of hole states and which serves often as a key component in modified continuum-based models to capture carrier localization effects in transport or optical gain calculations.

Polar InGaN/GaN quantum wells (QWs) have found widespread use as the active region of short wavelength range light-emitting diodes (LEDs).[1] To further improve the efficiency of these devices, a detailed understanding of the fundamental properties of InGaN-based QWs is crucial. One of these properties is the radiative recombination rate and its dependence on carrier density and temperature. The radiative recombination rate is often discussed in terms of the radiative recombination coefficient B of the so-called *ABC*-model. Recent experimental studies reveal a rather unusual behavior of B with temperature T, namely that it increases weakly with increasing T.[2] This behavior is very different from situations found in more conventional QW systems, such as GaAs-based structures, where B generally decreases with increasing T.[3] However, it is important to note that recent theoretical studies show that the electronic and optical properties of InGaN QWs are often very different from those of more conventional III–V systems.[4–6] It has been demonstrated, both in experiment and theory, that, especially at low temperatures, the electronic and optical properties of these wells are dominated by carrier localization effects.[7,8] Given that efficient radiative recombination in nitride-based LEDs is an important quantity in designing and optimizing such devices, it is crucial to understand its underlying physics in detail.

Thus, the evolution of B with temperature T has been targeted in several theoretical works, though their predicted trends vary noticeably.[6,9] Studies by Jones *et al.*,[6] applying a modified continuum-based model to account for carrier localization effects, found a reduction of B with increasing T. Recent atomistic theoretical investigations[9] report that the experimentally observed temperature dependence of B can be predicted correctly only when In atom clustering in the QW is introduced. However, the structural characterization of *c*-plane InGaN QWs shows very little evidence for this; rather, it points to a random distribution of In atoms (random alloy) in the well.[10,11] In Ref. 2, an empirical broadening of the hole density of states (h-DOS) is introduced to obtain an increase in B with T.

The above discussion highlights that even though alloy fluctuations are accounted for in theoretical models, their impact on the DOS, thus the energetic distribution of states, seems to be strongly dependent on the assumptions made. As a consequence, predicted trends may differ from experimental observations or assumptions

have to be made which are not necessarily consistent with the structural characteristics of InGaN QWs.

In this work, we show that the experimentally observed trend of increasing B with increasing temperature T is captured by our atomistic model without the assumption of In atom clustering and without treating the h-DOS as a free fitting parameter. Having calculated the h-DOS for InGaN QWs with In contents ranging from 5% to 25%, we extract the Stokes shift for the studied structures by evaluating absorption spectra and our previously obtained photoluminescence (PL) peak energies. The obtained Stokes shifts are compared to experimental data, showing good agreement. Moreover, we provide tail state energies, E_{tail}, which are often used to modify the DOS in transport or optical gain calculations of InGaN-based systems to account for carrier localization effects in continuum-based simulations.[12,13]

Our theoretical results are consistent with the anomalous T dependence of the B coefficient, but together with previous results,[14] they offer an explanation for this phenomenon in terms of carrier localization. These results show that it is important not only to account for those strongly localized states near the "band" edge but also to describe accurately the DOS away from the "band" edge and the whole ensemble of decreasingly localized states.

Our theoretical framework is based on a nearest neighbor sp^3 tight-binding (TB) model, which accounts for strain and built-in field effects via a valence field model and a local polarization theory; the framework is introduced in detail in Refs. 5 and 15. Overall, this model allows us to calculate the electronic structure of InGaN/GaN QWs with In contents varying from 5% to 25% on an atomistic level. The QW structures studied are based on the experimental systems discussed in Ref. 16, with further information given in Ref. 14. Due to the atomistic nature of our theoretical framework, it is necessary to specify the In atom distribution in the InGaN QW region. Consistent with experimental studies, a random distribution of In atoms in the QW is assumed.[10,11] Using this assumption, we find good agreement with experimentally obtained low temperature PL peak energies and full width at half maximum (FWHM) data over a wide range of In contents.[14]

Before turning to the radiative recombination rate and its unusual temperature dependence, we study the impact of carrier localization effects, due to random alloy fluctuations, on the h-DOS. This quantity is important to understand given that energetically higher lying states are populated with increasing temperature. In continuum-based models, to describe the electronic and optical properties of InGaN QWs, modifications to the h-DOS are often made *ad hoc*, treating the broadening of the DOS as a free fitting parameter.[2,12] In Ref. 2, an exponentially decaying h-DOS, similar to an Urbach tail,[17] has been assumed with a tail state energy, E_{tail}, as the free fitting parameter. To provide this information with our atomistic model, we calculate the h-DOS first and then extract E_{tail}. Thus, our data can be used in future (modified) continuum-based calculations of transport or optical gain calculations as an input.

To evaluate the h-DOS, 100 hole states have been calculated for 125 different microscopic configurations per In content (5%, 10%, 15%, and 25%), and the data have been collated and placed into energy bins of a fixed size of 30 meV; this number has been chosen to avoid having empty bins. The h-DOS is obtained by taking the derivative of the number of states per bin with respect to energy. Figure 1 shows, as an example, the calculated h-DOS for an InGaN/GaN QW with 25%
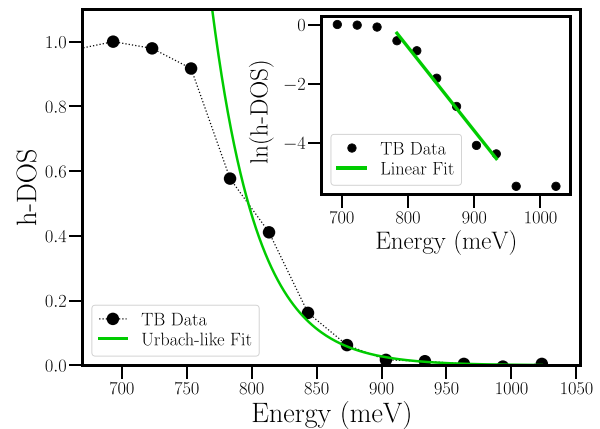

FIG. 1. Hole density of states (h-DOS) for an $In_{0.25}Ga_{0.75}N$/GaN well. Black circles: tight-binding data. Green solid line: fit to the data based on an Urbach-type model (see the main text for details). Inset: natural logarithm of the data from the main figure, indicating the region used for the fitting of the Urbach-type model. The zero of energy is the unstrained GaN valence band edge.

In. The TB data are denoted by the solid black circles and indicate a departure from the ideally "step-function"-like DOS of a homogeneous QW; the presence of tail states is observed for energies larger than approximately 750 meV. In all calculations, the zero of energy is the valence band edge of unstrained GaN. Random alloy fluctuations and resulting fluctuations in strain and (macroscopic and local) built-in potentials lead to the situation that the valence band edge varies with position across the QW structure; the h-DOS then includes a contribution from all these factors. For our analysis, primarily, the evolution of the h-DOS (shape of the curve) with energy is important. An Urbach like exponential decay of the h-DOS, which is assumed in many studies,[12] is confirmed through the plot of the natural logarithm of the data, as shown in the inset of Fig. 1. The TB data are again given by solid black circles, and the green solid line is a fit to the region in which the natural logarithm of the TB data changes linearly with energy (above 750 meV). From the slope of the solid green line, we extract the tail state energy E_{tail}. Using this information, the solid green line in the main part of Fig. 1 yields a very good description of the h-DOS calculated from our atomistic model. The same analysis has been carried out for all considered In contents and provides an equally good description (not shown).

Figure 2 displays the extracted tail state energies, E_{tail}, as a function of the In content, x, and reveals an increase in E_{tail} with increasing x. For the 25% In case, E_{tail} reaches a value of over 30 meV. However, even for the low 5% In content well, a tail state energy of around 10 meV is found. We also note that the rate of increase in E_{tail} in the 5%–15% In content range is larger than that in the 15%–25% In content range despite the In content difference being equal ($\Delta x = 0.1$). In order to estimate tail state energies for other In contents, we use $E_{tail}^f(x) = ax - bx^2$ to fit the TB data (solid black line), which gives a good description of the data.

While this analysis provides insight into the broadening of the h-DOS, it cannot be directly measured or validated against experimental data. However, the presence of tail states in the DOS leads to a broadening of the absorption spectrum, which is widely observed in
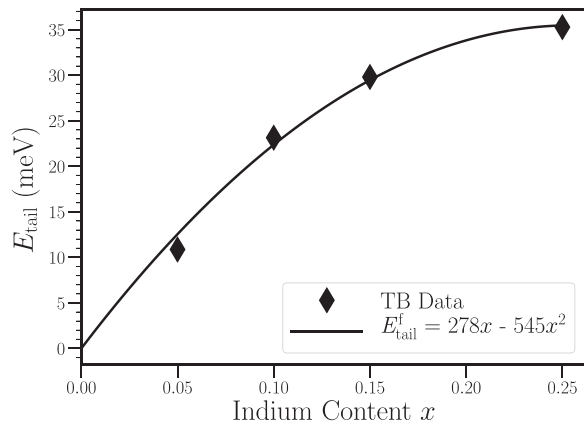
FIG. 2. Tail state energies E_{tail} as a function of the In content x in In$_x$Ga$_{1-x}$N/GaN quantum wells. The black diamonds are the tight-binding data, and the black solid line gives a fit, $E_{tail}^f = ax - bx^2$, with the coefficients a and b given in the figure.

experiment.[18–20] Thus, building on our calculations of the DOS, we evaluate the absorption spectra of our InGaN/GaN QWs via $\alpha'(h\nu) \propto \sum_{i,j} |d_{ij}^{e,h}|^2 \Theta(h\nu - E_{e,i} - E_{h,j})$,[21] where $E_{e,i}$ ($E_{h,j}$) is the electron (hole) eigenenergy of state i (j), $d_{ij}^{e,h} = e_0 \langle \psi_i^e | \mathbf{er} | \psi_j^h \rangle$ are the dipole matrix elements; here, e_0 is the elementary charge, $\mathbf{r}$ is the position operator, and $\mathbf{e} = 1/\sqrt{3}(1,1,1)$ is the light polarization vector. The dipole matrix elements have been directly calculated employing the TB wave functions.[22] The absorption spectrum $\alpha'(h\nu)$ is evaluated for each of the 125 different microscopic configurations per In content (5%, 10%, 15%, and 25%) using 100 electron and 100 hole TB states.

Figure 3 displays the final spectra, which are obtained by averaging over the 125 configurations per In content x. These spectra reflect the experimentally well-known broadening, which is often described by a sigmoidal function:[19,20] $\alpha'(h\nu) = \alpha_0 / \left(1 + e^{\left(\frac{h\nu - E_a}{E_u}\right)}\right)$. Here, E_u is the characteristic, or Urbach, tail energy and E_a is the absorption edge energy. Using the above expression to fit the TB data displayed in Fig. 3
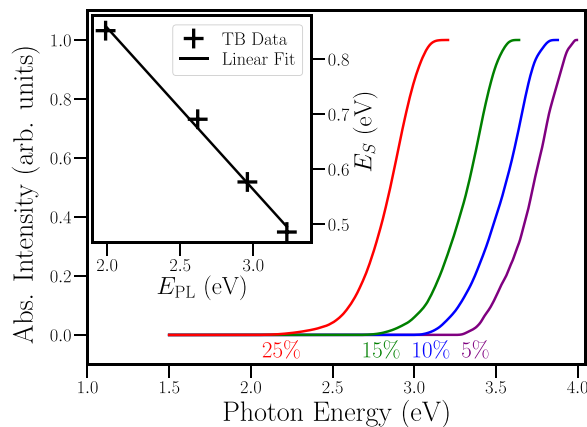
FIG. 3. Calculated absorption spectra for InGaN/GaN quantum wells with 5% (violet line), 10% (blue line), 15% (green line), and 25% (red line) In content. Inset: Stokes shift energies, E_s, as a function of the PL peak energies, E_{PL}.

enables the extraction of E_u and E_a as functions of the In content x. The obtained E_u and E_a values are summarized in Table I. E_u values on the order of 90–100 meV are found, which do not show much variation as In content, x, increases. The extracted absorption edge energies E_a decrease with increasing x, given that InN has a lower bandgap than GaN. Equipped with this information and having previously calculated (low T) PL peak energies E_{PL},[14] which are summarized in Table I, we can calculate the Stokes shift, E_s, as a function of In content, x, via $E_s(x) = E_a(x) - E_{PL}(x)$;[21] these results are presented in Table I. In the experimental study of Ref. 20, a Stokes shift energy of $E_s = 830$ meV is reported for a well with a PL peak energy of $E_{PL} = 1.96$ eV. The In$_{0.25}$Ga$_{0.75}$N QW studied here has a PL peak energy of $E_{PL} = 1.99$ eV and a Stokes shift of $E_s = 850$ meV, and thus, it is in good agreement with the experiment.[20] The experimentally observed linear increase in E_s with decreasing E_{PL} is reflected in our data (cf. inset of Fig. 3).

Having discussed the h-DOS, absorption spectra, and Stokes shifts of InGaN/GaN QWs for a wide In content range and thus the emission wavelength range, we now return to the discussion of the temperature dependence of the radiative recombination rate. To do so, the spontaneous emission rate, R_{sp}, is calculated as follows:[23]

$$R_{sp} = C \sum_{i,j} n(\lambda_{ij}) \left(E_i^e - E_j^h\right)^3 |d_{ij}^{e,h}|^2 f_i^e f_j^h, \qquad (1)$$

where the constant $C = \frac{4}{3} \frac{e^2}{\epsilon_0 c^3 \hbar^4}$, with c being the vacuum speed of light, ϵ_0 being the free space permittivity, and $\hbar$ being the reduced Planck's constant. Fermi functions for electrons and holes are denoted by f_i^e and f_j^h. The dipole matrix elements $d_{ij}^{e,h}$ are again directly calculated from the TB wave functions; E_i^e and E_j^h are TB eigenenergies of electron state i and hole state j. The wavelength/emission energy dependent refractive index $n(\lambda_{ij})$ is evaluated using a Sellmeier type description.[24] Once R_{sp} has been determined, we find the rate of spontaneous emission per in-plane area of the well, $r = R_{sp}/A_{QW}$. In order to compare our results with reported experimental data, we calculate the sheet radiative recombination coefficient $B_{2D} = r/np$, where n and p are the carrier densities for electrons (n) and holes (p), assuming that the material is electrically neutral ($n = p$). We note that for high carrier densities in the well, the electrostatic built-in field due to strain and piezoelectric polarization will be screened. This effect affects the wave function overlap and consequently the magnitude of B_{2D}. However, here we aim to understand and study the temperature dependence of the radiative recombination rate at a fixed and relatively low carrier density of $n = p = 1.2 \times 10^{12}$ cm^{-2}, which is motivated by the experiments in Ref. 2 (see also Ref. 9). Thus, field screening effects are expected to be of secondary importance for the present study.

TABLE I. Absorption edge energy (E_a), low temperature photoluminescence peak energy (E_{PL}), Urbach tail energy (E_u), and Stokes shift (E_s) for InGaN/GaN QWs with varying In contents extracted from a sigmoidal model. E_{PL} values have been taken from Ref. 14.

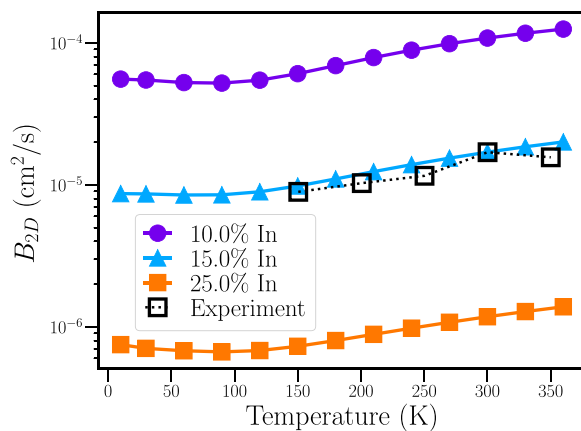| In content	E_a (eV)	E_u (meV)	E_{PL} (eV)	E_s (meV)
5%	3.72	95.5	3.23	490
10%	3.54	103.6	2.96	580
15%	3.31	98.3	2.62	690
25%	2.84	94.2	1.99	850

Figure 4 displays our calculated $B_{2D}(T)$ for QW systems with 10%, 15%, and 25% In, along with the experimental data from Ref. 2. Several factors are important to note when looking at the experimental data in comparison to our theoretical results. First, it should be noted that in the experimental study of Ref. 2, B_{2D} values are extracted by fitting A, B, and C coefficients simultaneously. Thus, different combinations of A and C values may affect the extracted B_{2D} values. On the theoretical side, we have not targeted the specific QW structures analyzed in Ref. 2 in terms of In content or well width. Therefore, a one-to-one comparison is not possible and not targeted. However, in general, the comparison between our theoretical results and the experimental data from Ref. 2 provides a good initial reference frame to investigate *trends* in the evolution of B_{2D} with increasing temperature T.

Overall, we find the expected trend that for a given temperature, B_{2D} decreases with increasing In content, x. This stems from two factors. First, considering the structures grown and studied in Refs. 14 and 16, the well width increases slightly with increasing x. Second, a higher In content leads to a stronger piezoelectric field. The combination of these two factors leads to a stronger quantum confined Stark effect and thus a stronger spatial separation of electron and hole wave functions, which reduces the spontaneous emission rate and thus B_{2D}.

Furthermore, Fig. 4 shows that for all three In contents, B_{2D} (slightly) increases with increasing T. The extremely good agreement between theory and experiment should be regarded as a coincidence, following our discussion on, for instance, the structural properties above. Nevertheless, given that independent of the In content considered in the calculations, the same trend is reflected, our theoretical model captures the main effects observed in the experiment. This result is achieved *without* assuming In atom clustering in the QW and so is in contrast to Ref. 9, where In atom clustering is *essential* to model an increasing B_{2D} with increasing T; in the random alloy case, the data in Ref. 9 show a *decrease* in B with increasing T. Our presented results are fully consistent with the experimental observation of a random In atom distribution in InGaN/GaN QWs while still predicting the experimentally observed trend of increasing B_{2D} with T.
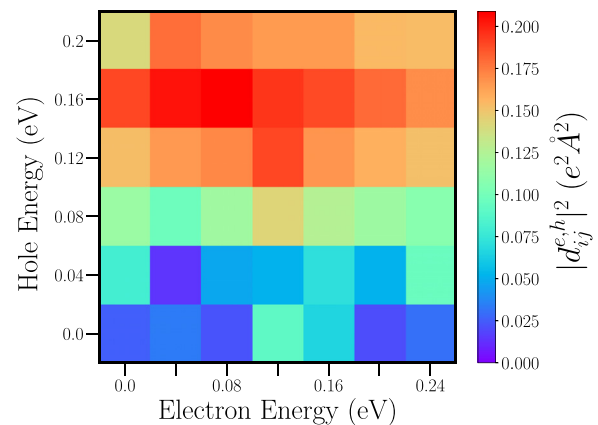
The cause of the above discussed trend in B_{2D} with T can be traced back to the changes in the magnitude of the dipole matrix elements between electron and hole states when populating energy levels further away from the "band" edges. Figure 5 displays $|d_{ij}^{e,h}|^2$ as a function of electron and hole state energies relative to the conduction and valence "band" edges; the In content in the well is 10%. The results from the 125 different configurations are collated and grouped into energy bins of width 40 meV and averaged over the number of elements in each bin. The bottom left corner of Fig. 5 corresponds to dipole matrix elements between states near the "band" edges, which are strongly localized states and which contribute mainly at low temperatures and carrier densities. Energetically higher lying states, exhibiting larger dipole matrix elements, are populated as T increases, thus resulting in the observed increase in B_{2D} with T in Fig. 4.

The above analysis shows that the unusual temperature dependence of B_{2D} stems from carrier localization and thus indicates that an accurate description of these effects is key. The description of alloy fluctuations and connected carrier localization effects may noticeably vary between different models, even within the same theoretical framework. In TB models, one factor is, for instance, how local built-in potential fluctuations are treated. TB models that include or exclude local field fluctuations may predict different carrier localization characteristics; these differences will be further compounded by differences in TB parameters.[14] Similar but also different aspects come into play in modified continuum-based models. Here, for example, the local In content is obtained by an averaging procedure.[6] This leads to a coarser spatial resolution in comparison to an atomistic model and may lead to different spatial localization characteristics and deviations in energies of the electron and hole states when compared to an atomistic model.

We also note that further studies are required to elucidate the temperature dependence of the radiative and also nonradiative recombination properties of InGaN/GaN QWs. For instance, the observed slight increase in B_{2D} with temperature may be dependent on the carrier density. With increasing carrier density, the localized states may then be occupied so that B_{2D} could become temperature independent. Furthermore, given that, in the experiment, B_{2D} is extracted by fitting A and C coefficients simultaneously, further investigations on, for

FIG. 4. Radiative recombination rate B_{2D} in $In_xGa_{1-x}N$/GaN wells as a function of temperature and alloy composition at a carrier density $n = p = 1.2 \times 10^{12}$ cm^{-2}: 10% In (purple filled circles), 15% In (blue filled triangles), 25% In (orange filled squares), and experiment from Ref. 2 (black open squares).

FIG. 5. Energy resolved dipole matrix elements $|d_{ij}^{e,h}|^2$ for the $In_{0.1}Ga_{0.9}N$/GaN well. Energies are given with respect to the band edges. More details are given in the main text.

instance, how C changes with temperature and carrier density are important.

In summary, we have studied the temperature dependence of the radiative recombination rate in terms of the B_{2D} coefficient. Both the temperature dependence and the magnitude of the B_{2D} coefficients calculated are in good agreement with literature experimental values. Our study reveals that the unusual temperature dependence of B_{2D} stems from the presence of an ensemble of localized states in InGaN QWs. Energetically higher lying, less localized, states, with larger dipole matrix elements, are populated by increasing the temperature; as a consequence, B_{2D} increases. We note that this finding is obtained without assuming In atom clustering in the QWs or by using the hole density of states as a fitting parameter. Given that the temperature dependence of the B_{2D} coefficient is tightly linked to modifications to the (hole) density of states, we have calculated Urbach tail energies for this quantity for InGaN QWs emitting over a wide wavelength range. Additionally, we have evaluated Stokes shifts in these systems. Comparison with experimental data shows good agreement, thus adding further trust that our model describes the modification of the density of states in InGaN QWs. Our results are thus consistent with experimental findings on both the optical (temperature dependence of B, Stokes shifts) and structural (random alloy configuration) properties of InGaN QWs and provide information, e.g., Urbach tail energies for hole density of states, which can be used in future modified continuum-based calculations.

The data that support the findings of this study are available from the corresponding author upon reasonable request.

REFERENCES

[1]C. J. Humphreys, MRS Bull. **33**, 459 (2008).

[2]F. Nippert, S. Y. Karpov, G. Callsen, B. Galler, T. Kure, C. Nenstiel, M. R. Wagner, M. Straßburg, H.-J. Lugauer, and A. Hoffmann, Appl. Phys. Lett. **109**, 161103 (2016).

[3]P. Blood, IEEE J. Quantum Electron. **36**, 354 (2000).

[4]D. Watson-Parris, M. J. Godfrey, P. Dawson, R. A. Oliver, M. J. Galtrey, M. J. Kappers, and C. J. Humphreys, Phys. Rev. B **83**, 115321 (2011).

[5]S. Schulz, M. A. Caro, C. Coughlan, and E. P. O'Reilly, Phys. Rev. B **91**, 035439 (2015).

[6]C. M. Jones, C.-H. Teng, Q. Yan, P.-C. Ku, and E. Kioupakis, Appl. Phys. Lett. **111**, 113501 (2017).

[7]S. F. Chichibu, A. Uedono, T. Onuma, B. A. Haskell, A. Chakraborty, T. Koyama, P. T. Fini, S. Keller, S. P. DenBaars, J. S. Speck, U. K. Mishra, S. Nakamura, S. Yamaguchi, S. Kamiyama, H. Amano, I. Akasaki, J. Han, and T. Sota, Nat. Mater. **5**, 810 (2006).

[8]P. Dawson, S. Schulz, R. A. Oliver, M. J. Kappers, and C. J. Humphreys, J. Appl. Phys. **119**, 181505 (2016).

[9]A. Di Vito, A. Pecchia, A. Di Carlo, and M. Auf der Maur, Phys. Rev. Appl. **12**, 014055 (2019).

[10]T. M. Smeeton, M. J. Kappers, J. S. Barnard, M. E. Vickers, and C. J. Humphreys, Appl. Phys. Lett. **83**, 5419 (2003).

[11]M. J. Galtrey, R. A. Oliver, M. J. Kappers, C. J. Humphreys, D. J. Stokes, P. H. Clifton, and A. Cerezo, Appl. Phys. Lett. **90**, 061903 (2007).

[12]B. Witzigmann, M. Tomamichel, S. Steiger, R. G. Veprek, K. Kojima, and U. T. Schwarz, IEEE J. Quantum Electron. **44**, 144 (2008).

[13]H. Morkoc, *Handbook of Nitride Semiconductors and Devices*, Volume 3: GaN-based Optical and Electronic Devices (Wiley-VCH, Weinheim, 2009).

[14]D. S. P. Tanner, P. Dawson, M. J. Kappers, R. A. Oliver, and S. Schulz, Phys. Rev. Appl. **13**, 044068 (2020).

[15]M. A. Caro, S. Schulz, and E. P. O'Reilly, Phys. Rev. B **88**, 214103 (2013).

[16]D. M. Graham, A. Soltani-Vala, P. Dawson, M. J. Godfrey, T. M. Smeeton, J. S. Barnard, M. J. Kappers, C. J. Humphreys, and E. J. Thrush, J. Appl. Phys. **97**, 103508 (2005).

[17]F. Urbach, Phys. Rev. **92**, 1324 (1953).

[18]M. Piccardo, C.-K. Li, Y.-R. Wu, J. S. Speck, B. Bonef, R. M. Farrell, M. Filoche, L. Martinelli, J. Peretti, and C. Weisbuch, Phys. Rev. B **95**, 144205 (2017).

[19]K. P. O'Donnell, R. W. Martin, and P. G. Middleton, Phys. Rev. Lett. **82**, 237 (1999).

[20]B. Damilano, N. Grandjean, J. Massies, L. Siozade, and J. Leymarie, Appl. Phys. Lett. **77**, 1268 (2000).

[21]D. T. S. Watson-Parris, "Carrier localization in InGaN/GaN quantum wells," Ph.D. thesis (University of Manchester, 2011).

[22]S. Schulz, S. Schumacher, and G. Czycholl, Phys. Rev. B **73**, 245327 (2006).

[23]Y.-R. Wu, Y.-Y. Lin, H.-H. Huang, and J. Singh, J. Appl. Phys. **105**, 013117 (2009).

[24]S. K. Patra, T. Wang, T. J. Puchtler, T. Zhu, R. A. Oliver, R. A. Taylor, and S. Schulz, Phys. Status Solidi B **254**, 1600675 (2017).